http://dx.doi.org/10.5012/bkcs.2011.32.12.4371

Growth Characteristics of Amorphous Silicon Oxide Nanowires Synthesized *via* Annealing of Ni/SiO_2/Si Substrates

Kwon Koo Cho, Jong Keun Ha, Ki Won Kim, Kwang Sun Ryu,† and Hye Sung Kim‡,*

School of Materials Science and Engineering, ERI and i-cube center, Gyeongsang National University, Jinju 660-701, Korea
†Department of Chemistry, University of Ulsan, Ulsan 680-749, Korea
*‡Department of Nanomaterials Engineering, College of Nanoscience & Nanotechnology, Pusan National University, Kyongnam 627-706, Korea. *E-mail: hsk@pusan.ac.kr*
Received June 21, 2011, Accepted October 18, 2011

In this work, we investigate the growth behavior of silicon oxide nanowires *via* a solid-liquid-solid process. Silicon oxide nanowires were synthesized at 1000 ºC in an Ar and H_2 mixed gas. A pre-oxidized silicon wafer and a nickel film are used as the substrate and catalyst, respectively. We propose two distinctive growth modes for the silicon oxide nanowires that both act as a unique solid-liquid-solid growth process. We named the two growth mechanisms "grounded-growth" and "branched-growth" modes to characterize their unique solid-liquid-solid growth behavior. The two growth modes were classified by the generation site of the nanowires. The grounded-growth mode in which the grown nanowires are generated from the substrate and the branched-growth mode where the nanowires are grown from the side of the previously grown nanowires or at the metal catalyst drop attached at the tip of the nanowire stem.

Key Words : Silicon oxide, Nanowires, Solid-Liquid-Solid, Vapor-Liquid-Solid, Growth behavior

Introduction

In the past decade, the one-dimensional nanostructure has received much attention not only because of its nanoscale size but also its novel properties, variable morphologies, and extraordinary applications.[1-4] Specifically, silicon-based nanowires, such as silicon (Si) and silicon oxide (SiOx) nanowires, have attracted attention for their potential in realizing nanosized devices such as semiconductors, blue light emitters, and optical sensors with high sensitivity.[5-8]

The growth mechanism of silicon-based nanowires is mostly described either by the vapor-liquid-solid (VLS) or solid-liquid-solid (SLS) process. The VLS and SLS mechanisms are very similar; the difference between them is in the phase of the silicon source material. The source material in the VLS growth mechanism is supplied to the vapor phase. On the other hand, that in the SLS growth mechanism is supplied to the solid phase. The VLS process was first described by Wagner and Ellis in 1964,[9] which was developed by Givargizov[10] in 1975. An SLS process derived from the VLS mode was first reported for obtaining amorphous silicon nanowires by Yan *et al*. in 2000.[11] They reported that amorphous silicon nanowires with an average diameter of 20 nm were synthesized at 950 ºC under an Ar/H_2 on a large area of a Ni-coated Si substrate without supplying any Si sources. Since then, many research groups in the fabrication of silicon-based nanowires have used the SLS process than VLS process due to simple fabrication process. The fabrication of silicon-based nanowires using the SLS growth mechanism can be summed up in only two steps; the coating of the catalyst on the silicon substrate and the heating of the catalyst-deposited silicon substrate in an inert gas atmosphere. Also, there was no additional source of silicon, except for a silicon wafer used as a substrate. However, there is a slight difference in the morphology, growth behavior, and growth mechanism of the resultant in accordance with the researchers, despite the simple and analogous experimental condition. For example, solid-solid (SS),[12] head-growth SLS[13] and solid-vapor-liquid-solid (SVLS)[14] mechanism were derived from SLS mechanism in order to express the exact growth behavior of silicon oxide nanowires. Although substantial progress has been made in the production more than a decade ago, the SLS growth mechanism is still poorly understood.

In this paper, we present the preparation and characterization of silicon oxide nanowires *via* the simple heating of Ni/SiO_2/Si substrate system in H_2:Ar mixture without any additional silicon source supply. We systematically investigated the effect of the synthesis time on the growth behavior and mechanism. This study, thus, attempts to improve the understanding of the growth behavior and mechanism of silicon-based nanowires by using only the SLS growth mechanism on the basis of strict experimental observations.

Experimental

The p-type silicon substrates with (100) orientation and 10 mm × 5 mm size were rinsed clean in a sonicating bath of acetone and ethyl-alcohol for approximately 20 min, followed by a second rinsing under running deionized water. The cleaned silicon substrates were dried in a dry oven of 50 ºC. Next, the dried substrates were put into a horizontal tube furnace to form a silicon dioxide (SiO_2) layer. After thermally oxidizing the silicon substrates at 1100 ºC under 50 sccm oxygen gas for 30 min, about 80 nm in thickness of the Si

substrate surface was changed into a silicon oxide (SiO_2) layer. Ni films of about 50 nm were deposited on the oxide layer by DC magnetron sputter (200 V and 0.1 A in voltage and current). Figure 1 shows the Ni-coated Si substrate used in this work. The substrate was put on an alumina plate and then put in the center of a horizontal quartz tube of 45 mm in diameter and 1,000 mm in length. The synthesis was carried out at 1000 °C in an H_2:Ar (100:200 sccm) mixture gas with varying reaction times (0-60 min). An Ar gas (99.99%) of 200 sccm was flowed into the quartz tube throughout the heating process. In addition, H_2 gas was supplied manually by turning on/off the valve on the heating equipment when the fabricating started and finished. The reaction time was determined by the input duration time of H_2 gas after increasing the temperature until reaching the synthesis temperature (1000 °C) under Ar gas. During the growth procedure, the furnace was maintained under ambient pressure. After cooling down to room temperature, a white-gray product was found on the surface of the silicon substrates.

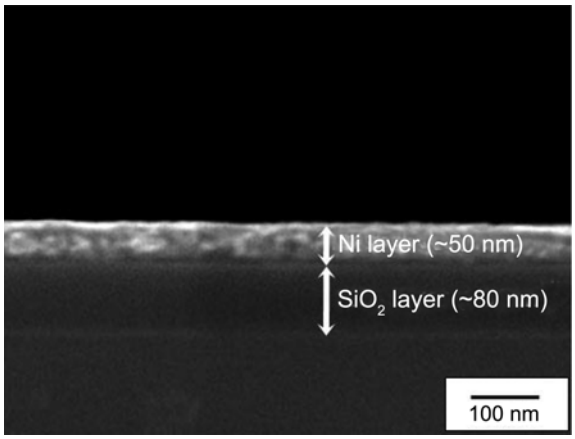

Figure 1. Ni-coated and pre-oxidized silicon substrate used in this work.

The products were characterized by FE-SEM equipped with an energy-dispersive X-ray spectroscope (EDX) and TEM.

Results and Discussion

Figure 2 is low-magnified FE-SEM images showing growth process of nanowires with synthesis time. Figure 2(a) shows the Ni catalysts observed after increasing the temperature to 1000 °C in only argon gas (or just before the input of H_2 gas). The Ni thin film shown in Figure 1 was changed to microislands with very rugged surface morphology and average diameters of around 1 um as shown in Figure 2(a). We guessed that each crystallite agglomerate in the catalysts contained several well-shaped nanocrystallites. Meanwhile, the surface of substrate in Figure 2(a) was even and clean. Figures 2(b) and (c) show the FE-SEM images of the samples synthesized for 2 and 4 min. Although some nanowires had straight or smoothly curved morphology, most nanowires exhibited a tangled and curved morphology. In addition, we were able to observe the surface of the substrates in Figures 2(b) and (c) because the grown amount was small. The surface shown in Figures 2(b) and (c) was very rugged contrary to that shown in Figure 2(a). As indicated by the arrow in Figure 2(c), a new area with a leaf pattern appeared on the surface. There were also many flower-like nanostructures with petals or sepal shapes as marked by the arrow in Figure 2(b). Nanowires with a straight or smoothly curved morphology abruptly appeared in the sample synthesized for 10 min (Fig. 2(d)). The amount of straight nanowires increased as the synthesis time increased, as shown in Figures 2(d)-(f). Also, the nanowires synthesized more than 10 min have a smooth surface and uniform diameter of average 40 nm regardless of synthesis time. The flower-like nanostructures, surface morphology and droplet mentioned in Figure 2 will be specifically discussed in Figures 4 and 5 with high magnified images and composition analysis.

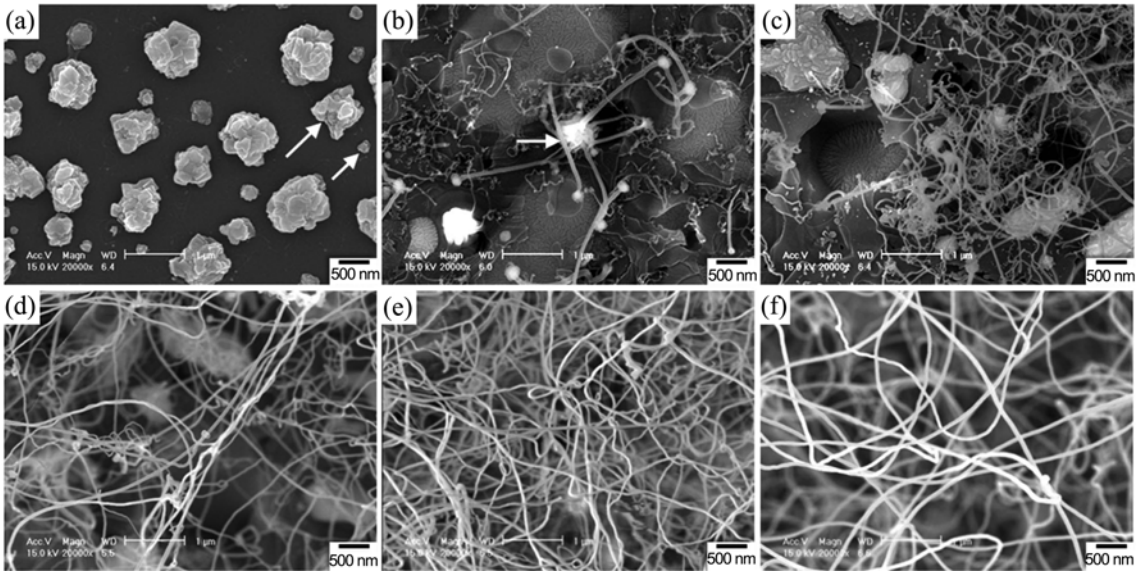

Figure 2. FE-SEM images showing silicon oxide nanowires prepared with varying synthesis times; (a) 0 min, (b) 2 min, (c) 4 min, (d) 10 min, (e) 30 min and (f) 60 min (low magnification top-view).

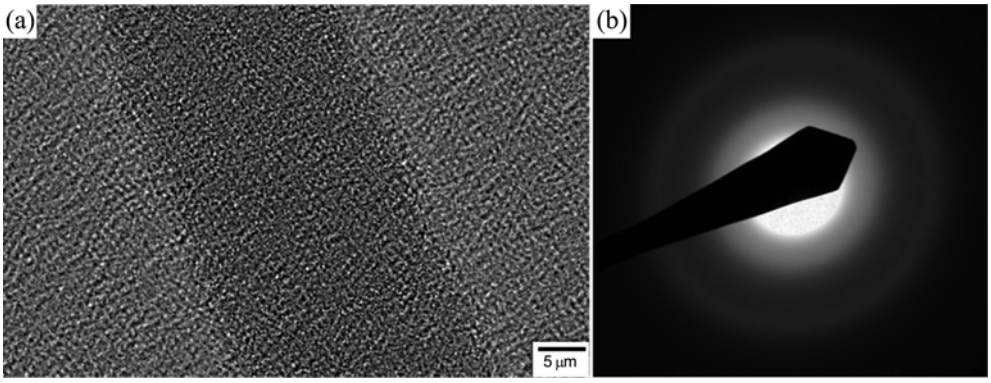

Figure 3. (a) TEM micrograph and (b) electron diffraction pattern of nanowires synthesized for 30 min. EDX analysis revealed that the composition of the nanowire is ~$SiO_{1.9}$.

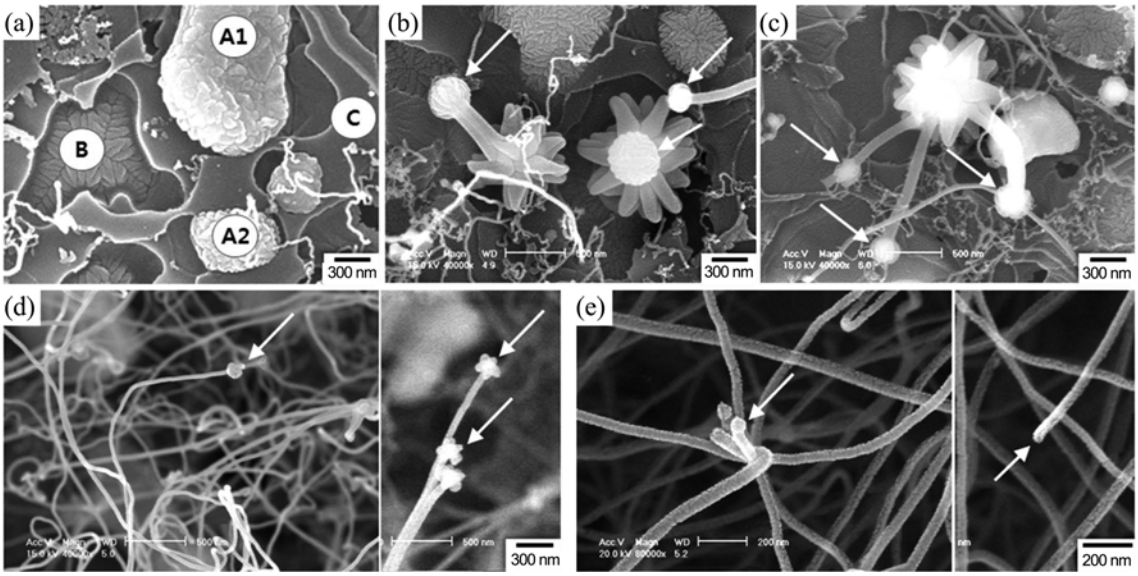

Figure 4. FE-SEM images of nanowires, catalysts and substrates with different synthesis times at 1000 °C; (a)~(c) 2 min, (d) 10 min, and (e) 30 min. These are important images to understand the generation and growth behavior of silicon oxide nanowires.

Figure 3 shows a TEM micrograph and electron diffraction pattern of nanowire taken in sample synthesized for 30 min. As reported in the previous works,[15,16] the TEM analysis of the nanowire indicates that it is amorphous and silicon oxide. The composition is predominately $SiO_{1.9}$ as measured by energy dispersive spectroscopy. Accordingly, we use the term "silicon oxide nanowires" in to represent the nanowires grown in this work.

Figure 4 shows the high-magnified FE-SEM images taken from the samples synthesized for 2(a, b, c), 10 (d) and 30 (e) min shown in Figure 2. Figure 4(a) is of the FE-SEM images showing the morphology of the substrate surface observed after a synthesis time of 2 min. The surface could be classified by three parts including catalysts (marked by A1 and A2), a leaf pattern (marked by B), and a plateau area (marked by C). A1 and A2 are big and small catalysts, respectively. The images clearly show that the catalysts sank inside the substrate. Particularly, the small catalyst (A2) nearly sank inside the substrate. On the other hand, the morphology with the leaf pattern was observed in the area marked by B, which perfectly sank beneath the surface. Lastly, the C area was very even and had a network structure, which may be the silicon substrate. Many flower-like nanostructures were observed in the initial synthesis step as shown in Figures 4(b) and (c). The big droplets marked by arrows in Figures 4(b) and (c) consist of very small nanoparticles like a true blossom. From the detailed FE-SEM analysis, we observed that the flower-like nanostructures were growing like actual flowers with the synthesis time. The nanostructures depicted in Figures 4(a)-(c) will be discussed again in detail with EDX analysis in Figure 5. In Figures 4(b), (c), (d), and (e), the nanowires have droplets at the end of the stem. Also, we can observe the morphology and size variation of the droplets attached at the tip of the stems. The diameter of the droplets decreased with increasing synthesis time. The average diameter of droplets measured from the samples synthesized for 2 (b and c), 10 (d), and 30 min (e) are around 400, 200, and 80 nm, respectively. As mentioned above, the droplets consisted of nanoparticles of a very small size. We could not count the

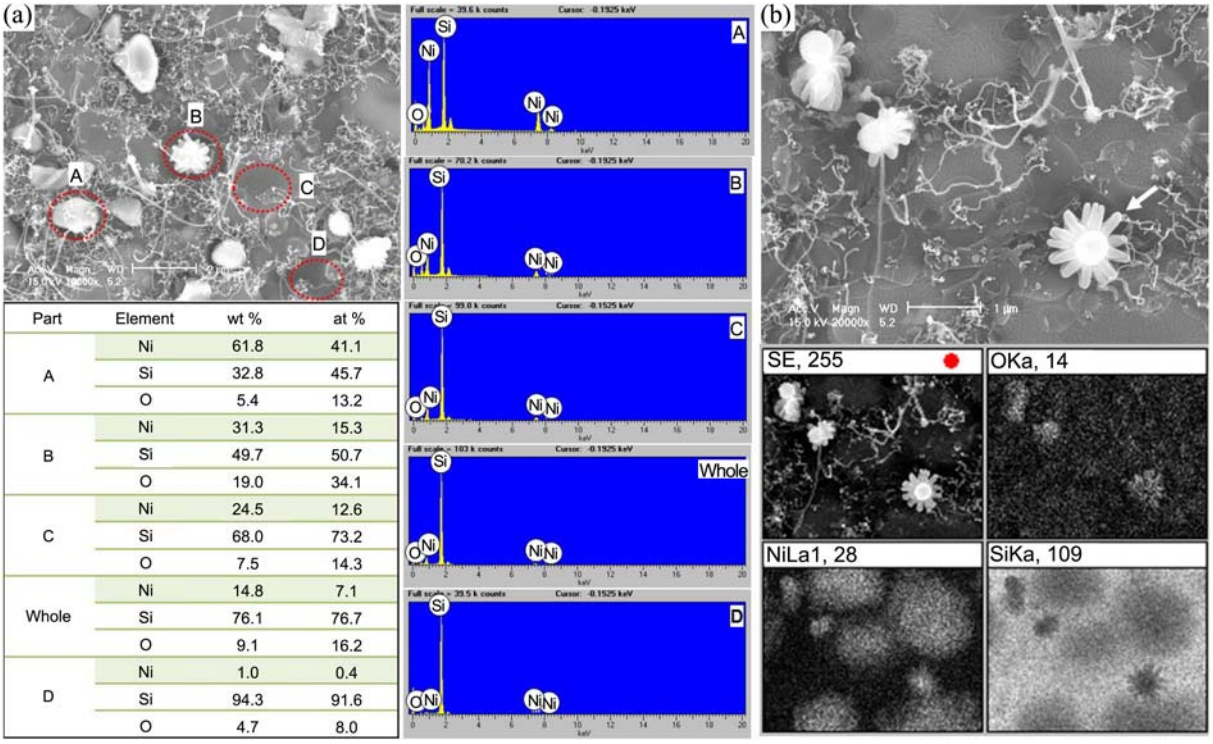

Part	Element	wt %	at %
A	Ni	61.8	41.1
	Si	32.8	45.7
	O	5.4	13.2
B	Ni	31.3	15.3
	Si	49.7	50.7
	O	19.0	34.1
C	Ni	24.5	12.6
	Si	68.0	73.2
	O	7.5	14.3
Whole	Ni	14.8	7.1
	Si	76.1	76.7
	O	9.1	16.2
D	Ni	1.0	0.4
	Si	94.3	91.6
	O	4.7	8.0

Figure 5. (a) FE-SEM images and EDX spectra, and (b) EDX mapping of important parts taken from the sample synthesized at 1000 °C for 2 min.

number of nanoparticles within the droplets indicated by the arrows in Figures 4(b) and (c) because the nanoparticles were extremely small and numerous; thus, the boundaries between nanoparticles was uncertain. On the other hand, we could count the number of nanoparticles within the droplets in the two samples synthesized for 10 and 30 min in Figures 4(d) and (e). The number of nanoparticles within the droplets of sample synthesized for 10 min was around 4-7 (Fig. 4(d)). The number in 30 min synthesis time was only one or none (Fig. 4(e)). Namely, the number of nanoparticles within the droplets dramatically decreased as the synthesis time increased. We will discuss the flower-like nanostructures, the morphology change of the substrate surface, the change of nanoparticles number within droplets, and so on from a perspective that will enable us to understand the generation and growth behavior of the silicon oxide nanowires. We suggest that these will be used valuable clue for comprehending the growth behavior of nanowires in Figures 6 and 7.

Figure 5 shows the FE-SEM images and EDX spectrum analysis results on the important parts shown in Figures 4(a)-(c). The parts marked by A, B, C, and D in Figure 5(a) are catalyst, flower-like nanostructure, leaf pattern and plateau, respectively. The "whole" in composition table of Figure 5(a) means total area shown in FE-SEM image of Figure 5(a). The EDX spectrum and chemical composition of the four parts and the total area are shown in Figure 5(a). The EDX spectrum on each part indicates only three signals of Ni, Si, and O. The five parts in the chemical composition table and EDX spectrum of Figure 5(a) are sequenced in nickel content order used as catalyst in this work. The nickel contents of A, B, C, whole, and D parts are around 62, 31, 24, 14, and 1 wt. %, respectively. From this EDX analysis, we suggest that the A and D parts, on the basis of morphology and nickel content, are the catalyst and substrate, respectively. The B (flower-like) and C (leaf pattern) parts comprise abundant Ni. This fact suggests that Ni may play a key role in the formation of the B and C parts. We suggest that C part with leaf pattern is a Ni-Si alloy region formed by the interdiffusion between the catalyst and the silicon substrate. There are three flower-like nanostructures in the FE-SEM image of Figure 5(b). The flower-like nanostructure marked by the arrow is very similar to a cosmos. A more detailed component investigation of the flower-like nanostructures carried out through EDX mapping is shown in Figure 5(b). From the EDX mapping results, we confirmed that the flower-like nanostructures consisted of Ni and O. However, it was difficult to understand how the Ni catalysts were transformed to the flower-like nanostructures; therefore, this work is still in progress.

Figures 6(a) and (b) are FE-SEM images showing nanowires generated on the catalyst and leaf pattern part, respectively. The catalyst in Figure 6(a) will be transformed into the morphology of a leaf pattern (Fig. 6(b)) due to the interdiffusion between the Ni catalyst and Si substrate as the results shown in Figures 4(a) and 5(a). Namely, the nanowires shown in Figures 6(a) and (b) had the same generation site, which is catalyst. Also they have the catalysts not only at the bottom but also at the top of the nanowires. Figure 6(c) is the FE-SEM image showing the nanowires grown on the substrate surface of the sample synthesized for 30 min.

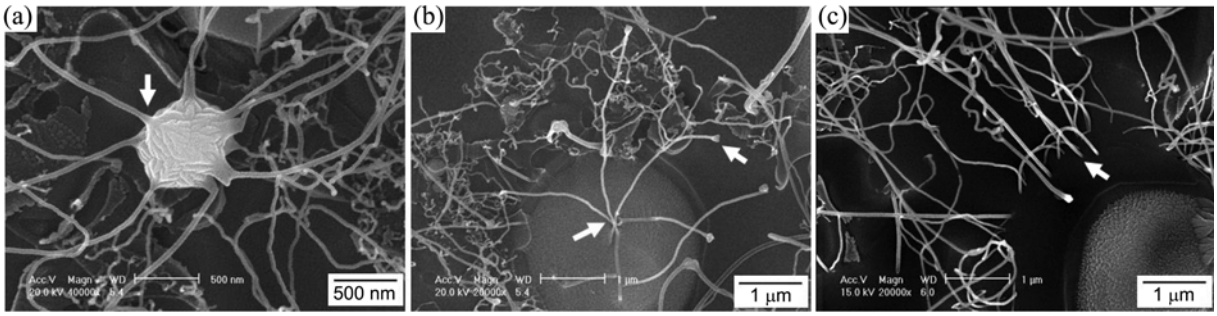

Figure 6. FE-SEM images showing various morphologies of silicon oxide nanowires grown on the substrates; (a) and (b) 4 min, and (c) 30 min.

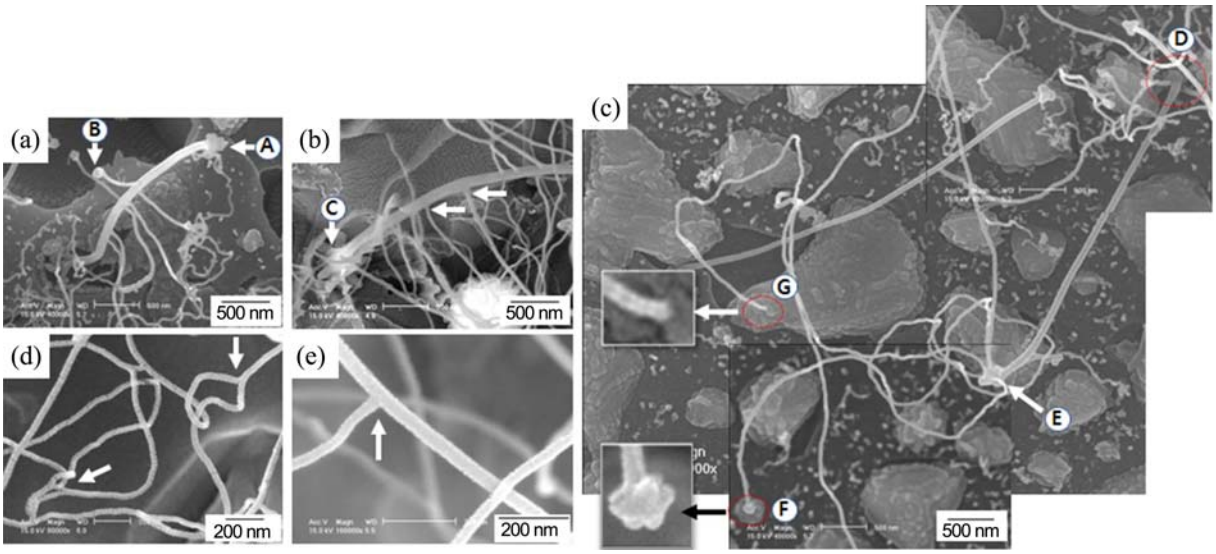

Figure 7. FE-SEM images showing various morphologies of silicon oxide nanowires grown from the side of the nanowires and from catalysts suspended over substrates; (a), (b) and (c) 4 min, and (d) and (e) 30 min.

Figure 6(c) looks as if there were no catalysts at the bottom of the nanowires unlike Figures 6(a) and (b), but we suppose that not the catalyst is to be seen at the bottom of the nanowires due to fully diffusion of nickel catalyst inside Si substrate at the high temperature for a long time. Anyway, the nanowires were fixed to the substrate. Thus, we named the growth mode "*grounded-growth mode*". Meanwhile, the existence of a solidified spherical droplet on the top of the nanowires is generally considered to be evidence of the operation of the VLS mechanism. On the other hand, the existence of the catalyst at the bottom of the nanowires illustrates that the growth mechanism is SLS. If so, the catalyst in this work should exist only at the bottom of nanowires because the synthesis process was typically the process of the SLS growth mechanism. However, such criteria for judgment of growth mechanism is not always so. Yan[11] and Duraia[17] reported the formation of silicon-based nanowires with the catalyst at the bottom of the nanowires, and the growth was explained by using the SLS mechanism. On the other hand, Lee[12] and Hsu[13] reported the growth of silicon-based nanowires with the catalyst at the top of the nanowires *via* the process of the SLS growth mechanism. The catalysts in this work existed not only at the bottom but also at the top of the nanowires, as can be seen in Figure 6. It appears as though a mixture of SLS and VLS mechanisms was operated. However, there were no grounds for the operation of the VLS growth mechanism in this work. The catalyst droplets with an average diameter of 1 um were formed (Fig. 2(a)), and they had a cluster shape made up of several small particles. The growth of the silicon oxide nanowires in the present study can be divided into four steps including the formation of Ni/Si droplets, continuous diffusion of Si atom, saturation and precipitation of Si atom within the droplets, and growth of silicon-based nanowires. We assume that the small particle within the big catalyst droplet was released back to the big catalyst droplet. The small particle was then gradually lifted off during the growth of the nanowires, as shown in Figures 6(a) and (b). For the first time, we show that a catalyst can simultaneously be at the top and bottom of the stem of nanowires synthesized using SLS mechanism.

Figure 7 is a series of FE-SEM images showing the morphology of some nanowires generated from the side of previously grown nanowires (Figs. 7(a), (b), (d) and (e)) or at the drop attached at the tip of the stem (Fig. 7(c)). As indicated by arrows in Figure 7(a), a big catalyst droplet is at

the tip of the main stem (marked A), and a small one is at the tip of the stem generated from the side of the main stem (marked B). Several branches with catalyst droplets at the tips and smooth morphologies were generated from the main stem. In Figure 7(b), the petal-like nanostructures shown in Figure 4(b) existed at the bottom of main stem (marked C). From the results of Figures 7(a) and (b), we proffer that the flower-like nanostructures grew with the progression of the synthesis time, and some nanoparticles were separated from the main catalyst droplet during the growth process, and then the separated nanoparticles played the catalyst in the growth of the branching nanowires generated from the side of the main stem. We often observed branching growth behavior during the initial synthesis step. Figure 7(c) is an FE-SEM image showing another branching growth behavior. The main stem was generated at the D position of the substrate surface, and the main stem had a big catalyst at its tip (marked E). Four or five nanowires were generated at the catalyst marked by E, and they had a catalyst (marked F) or nothing (marked G) at the tip. The thickness of the branched nanowires is around 30-50 nm and is similar to that of the nanowires synthesized for 30 min (Figs. 7(d) and (e)). We frequently observed one nanowire splitting into two nanowires, as indicated by the arrows in Figures 7(d) and (e), and the thickness of the nanowires barely changed when comparing before and after the split. As shown in Figure 7, many nanowires generated from the side of the previously grown nanowires (Figs. 7(a), (b), (d) and (e)) or at the droplet attached at the tip of the nanowire stem (Fig. 7(c)). We named the growth mode in this instance "*branched-growth mode*".

Conclusion

In summary, silicon oxide nanowires were synthesized through the simple heating of a $Ni/SiO_2/Si$ substrate in Ar and H_2 mixed gas. In order to observe the growth behavior and mechanism, FE-SEM analysis was intensively carried out in the initial synthesis step. Many nanowires with a curved morphology were formed during the initial synthesis time. Furthermore, nanowires with a smooth morphology abruptly increased from the synthesis time of 10 min, and we could not see the surface of the substrate through the FE-SEM in the sample synthesized for 30 min due to the abundance of nanowires. The thickness of the nanowires in the sample prepared for 10 min was around 30-50 nm, and that was not nearly varied by increasing synthesis time. Two distinctive growth modes of the silicon oxide nanowires were identified in this work. Some nanowires were generated on the substrate. On the other hand, some nanowires were generated from the side of previously grown nanowires or on the catalyst attached at the tip of the nanowire stem. In the present experiment, the silicon substrate only served as the silicon source. Therefore, the experiment condition in this work is a synthesis process for the conventional SLS growth mechanism. However, the growth mechanism shown in this work is slightly different from the conventional SLS mechanism. Therefore, we named the two growth mechanisms the "*grounded-growth*" and "*branched-growth*" modes as unique solid-liquid-solid growth behavior.

Acknowledgments. This research was supported by the National Research Foundation of Korea (NRF) grant funded by the Korea govemment (MEST) (No. 2010-0027664) and second stage of BK21.

References

1. Morales, A.; Lieber, C. M. *Science* **1998**, *279*, 208.
2. Pan, Z. W.; Dai, Z. R.; Wang, Z. L. *Science* **2001**, *291*, 1947.
3. Xia, Y.; Yang, P.; Sun, Y.; Wu, Y.; Mayers, B.; Cates, B.; Yin, Y.; Kim, F.; Yan, H. *Adv. Mater.* **2003**, *15*, 353.
4. Favier, F.; Walter, E. C.; Zach, M. P. O.; Benter, T.; Penner, R. M. *Science* **2001**, *293*, 2227.
5. Bogue, R. W. *Sens. Rev.* **2004**, *24*, 253.
6. Yu, D.; Hang, Q.; Ding, Y.; Zhang, H.; Bai, Z.; Wang, J.; Zou, Y.; Qian, W.; Xiong, G.; Feng, S. *Appl. Phys. Lett.* **1998**, *73*, 3076.
7. Wang, N.; Tang, Y. H.; Zhang, Y. F.; Lee, C. S.; Bello, I.; Lee, S. T. *Chem. Phys. Lett.* **1999**, *299*, 237.
8. Cui, Y.; Lieber, C. M. *Science* **2001**, *291*, 851.
9. Wagner, R. S.; Ellis, W. C. *Appl. Phys. Lett.* **1964**, *4*, 89.
10. Givargizov, E. I. *J. Cryst. Growth* **1975**, *31*, 20.
11. Yan, H. F.; Xing, Y. J.; Hang, Q. L.; Yu, D. P.; Wang, Y. P.; Xu, J.; Xi, Z. H.; Feng, S. Q. *Chem. Phys. Lett.* **2000**, *323*, 224.
12. Lee, K. H.; Yang, H. S.; Baik, K. H.; Bang, J.; Vanfleet, R. R.; Sigmund, W. *Chem. Phys. Lett.* **2004**, *383*, 380.
13. Hsu, C. H.; Chan, S. Y.; Chen, C. F. *Jpn. J. Appl. Phys.* **2007**, *46*(11), 7554.
14. Djamila, H.-B.; Pierre, P. *C. R. Chimie* **2007**, *10*, 658.
15. Zhang, J. G.; Liu, J.; Wang, D.; Choi, D.; Fifield, L. S.; Wang, C.; Xia, G.; Nie, Z.; Yang, Z.; Pederson, L. R.; Graff, G. *J. Power Sources* **2010**, *195*, 1691.
16. Srivastava, S. K.; Singh, P. K.; Singh, V. N.; Sood, K. N.; Haranath, D.; Kumar, V. *Physica E* **2009**, *41*, 1545
17. Duraia, E. M.; Mansurov, Z. A.; Tokmolden, S.; Beall, G. W. *Physica B* **2010**, *405*, 1176.